CONFLATION OF THERMAL BRIDGING ASSESSMENT AND BUILDING THERMAL SIMULATION

*Abdullatif E. Ben-Nakhi, **Essam O. Aasem
* College of Technological Studies, P.O. Box 3665, 22037, Salmiya, Kuwait
** Kuwait Institute for Scientific Research, P.O. Box 24885, 13109 Safat, Kuwait

ABSTRACT

The legislation and energy awareness have lead to increased thermal insulation levels in buildings. Consequently, heat flow, between the indoor and outdoor environments, due to thermal bridging is forming an increasing fraction of building thermal load. Accurate thermal bridging assessment is becoming more important not only to predict the heat flow, but also to predict the level of condensation and mould growth in the heating season. This paper presents a thermal bridging assessment module that is integrated within a state-of-the-art, whole building simulation environment in order to have more pragmatic boundary conditions.

INTRODUCTION

In general, heat flow through building construction is one-dimensional (i.e., in the direction perpendicular to the surface). This is because thermal conductance, and temperature differential in the perpendicular direction is much greater than that in the lateral directions. However, localized multi dimensional heat conduction through building envelope is common. Thermal bridge is the part of building envelope through which heat conduction is multi dimensional.

The multi dimensional character of heat conduction affects the local temperature distribution and heat flow rate. In other words, thermal bridging will bring the internal surface temperature nearer to the other side environment, and causes higher heat flow between the two environments. While the internal surface temperature should be considered in mould growth and condensation risk assessments during the heating season, higher heat flow rate should be taken into account during the design of buildings and their year round environmental control systems.

In general, buildings have several thermal bridges, which occur due to one or more of the following causes:

1- Change in thermal properties of building envelope in the lateral direction.

2- Change in construction thickness (e.g. a window within a wall).

3- Difference between internal and external areas (e.g. edges and corners).

4- Heat generation within building construction (hot water pipe).

In addition, the legislation and energy awareness have lead to increased insulation levels in buildings, which implies increased thermal resistance in the perpendicular direction. Consequently, the difference between thermal conductance in the perpendicular and lateral directions is reduced, which increases the potential for multi dimensional heat conduction in building constructions. Furthermore, the severity of the thermal bridging due to the causes mentioned above has increased.

Traditionally, facilities available to designers for assessing thermal bridging have involved either the use of guidebooks or general-purpose numerical analysis tools. The former suffers from the handicap that the design details in question does not necessarily match the details in the guidebooks. The latter can be time consuming to set up, unable to model multiple dynamic boundary conditions for a domain, and are not integrated with other heat transfer processes in the building.

There have been several recent initiatives aimed at improving this situation. Strachan et al (1995) introduced two such developments: the KOBRA software, which allows for 2D thermal bridge analysis, and the 3D conduction capabilities within an existing building energy simulation package. The former combined with the EUROKOBRA database, consisting of some 3000 thermal bridge details, provide a user-friendly way to analyse such thermal bridges. Although this method simplified domain

definition, the problem of boundary conditions was not tackled. The later tool facilitates multi-dimensional modeling of heat conduction through building construction. The gridding flexibility of this tool is inherited from the adopted unstructured[1] mesh, which has some shortcomings such as high CPU effort and space.

Accordingly, the current project was invoked in order to develop an adaptive thermal bridging assessment tool. This was achieved by incorporating structured 3D dynamic conduction capabilities into an existing building energy simulation environment. After introducing the theoretical background, the integration of the module into a state-of-the-art building simulation package is presented. Then, the numerical and analytical validation of the developed tool is presented. Finally, conclusions are given.

THEORETICAL BACKGROUND

Usually, heat conduction occurring in buildings is transient. That is because of the changing boundary conditions, which is affected by the outside climate, plant operation, occupants activity, etc. The differential equation of heat conduction can be written as

$$\rho \cdot c_p \frac{\partial T(\vec{r},t)}{\partial t} = -\sum_{i=1}^{N_b} \nabla \cdot \vec{q}_i + g(\vec{r},t) \qquad (1)$$

Many methods for the numerical formulation of the above equation exist. The control volume approach was adapted in the present work because of its physical elegance, and its formulation simplicity and flexibility. In addition, there are several possible schemes for the positioning of control volumes and their associated grid points. The approach adopted in the current work is based on putting one node on each material or boundary interface. Then positioning additional nodes in between according to the required resolution. After that, the control volume surfaces are located midway between grid points. This approach ensures continuity in the boundary conditions throughout each control volume surface, and continuity in the thermal conductance between nodes.

[1] In unstructured mesh the identification of grid points should be individually specified and they are not associated with an orderly defined grid lines.

The control volume formulation is achieved by integrating the associated partial differential equation (Eqn. 1) over a small control volume. Accordingly, for a rectangular parallelepiped control volume, with heterogeneous material and uniform boundary at each surface we have

$$\sum_{i=1}^{N_m} \rho_i \cdot c_i \cdot V_i \frac{\partial T}{\partial t} = \sum_{s=1}^{6} A_s \cdot q_s + V \cdot \bar{g} \qquad (2)$$

Where the heat flux q_s can be due to heat conduction, convection, or radiation, which are defined by

$$q_{cond} = \frac{\lambda_{j \to i} \cdot (T_j - T_i)}{\Delta x_{j \to i}} \qquad (3)$$

$$q_{conv} = h_c \cdot (T_j - T_i) \qquad (4)$$

$$q_{rad} = h_r \cdot (T_j - T_i) \qquad (5)$$

Based on the foregoing theory a structured 3D-gridding scheme has been developed. The main advantage of this scheme is that it enables localized 3D modeling. For example, a building can be modeled as a 1D problem except for parts of it that are represented by 3D model. The integration of the new scheme within a state-of-the-art simulation environment in presented in the next section.

IMPLEMENTATION

It is out of the scope of this paper to present the theory behind the building energy simulation represented here by the ESP-r (Clarke 1985), which is well established and reported in great detail elsewhere. However, a brief description of the ESP-r environment is necessary to present the implementation of the developed scheme within ESP-r.

The ESP-r is a tool for the transient simulation of heat and fluid flow within combined building/plant systems with control imposed. The structure of ESP-r is shown in Figure 1. By means of Project Manager, a simulation problem is defined by a set of data files whose names and locations are saved in a single system configuration file. By defining the system configuration file name to the Simulator, it will represent the problem by its equivalent network of time dependent thermal resistances and capacitances subjected to dynamic potential differences.

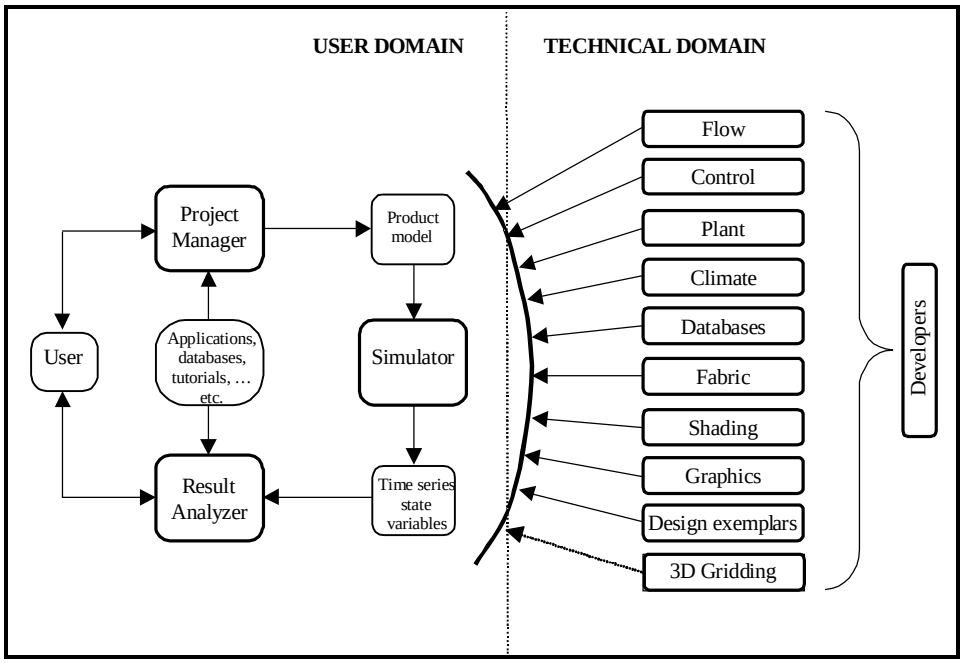

Figure 1: The ESP-r system (Clarke 1994)

By performing a simulation, the Simulator creates a result file that is analyzed by the Results Analyzer.

Accordingly, three levels of integration between the developed scheme with the ESP-r environment are considered. These levels are problem definition, simulation, and result analysis (Figure 2). Since ESP-r is equipped with an advanced gridding module called *grd*, the required data for the structured 3D scheme are defined within *grd*. However, the 1D problem should be defined within the ESP-r environment first.

The developed scheme deals with one zone at a time. Each zone is divided into local components and one imported domain. The local components are the default 1D constructions, which can be set to defined or not defined. The undefined local components are those components that will be represented by the imported domain. Therefore, in order to model 3D-heat flow through, say, the East and South walls, they should be set to undefined local components and a 3D model of the two walls and the edge in between should be defined and imported.

The imported domain is defined with respect to a cartesian coordinate system. The definition of the imported domain requires three sets of data: grid data, material geometry, and boundary conditions. The required grid data for the imported domain are the employed length unit (e.g. mm or cm), number of gridding lines, and distance between each two successive grid lines in each dimension. This group of grid data facilitates high level of gridding flexibility. The internal and external boundaries are referenced to existing boundaries in the 1D problem. Similarly, the thermo-physical properties of the imported domain are defined by referencing to existing layers within the 1D building constructions.

In order to encourage the usage of the developed scheme, it is furnished with the default ESP-r interface for the definition of the imported domain. Beside that, on-line help and exemplar are also provided.

The simulation of a problem within the Simulator is performed in a three-stage process: discretisation of the problem, derivation of the simulation equation for the nodal system, and simultaneous solution of the derived characteristic equations. The default ESP-r space discretisation approach is based on 1D heat conduction through building constructions. Accordingly, each inter-constructional node has two heat conduction connections. However, construction surface nodes have only one conduction connection. Depending on the boundary conditions, the other connections for the construction surface node are defined. For example,

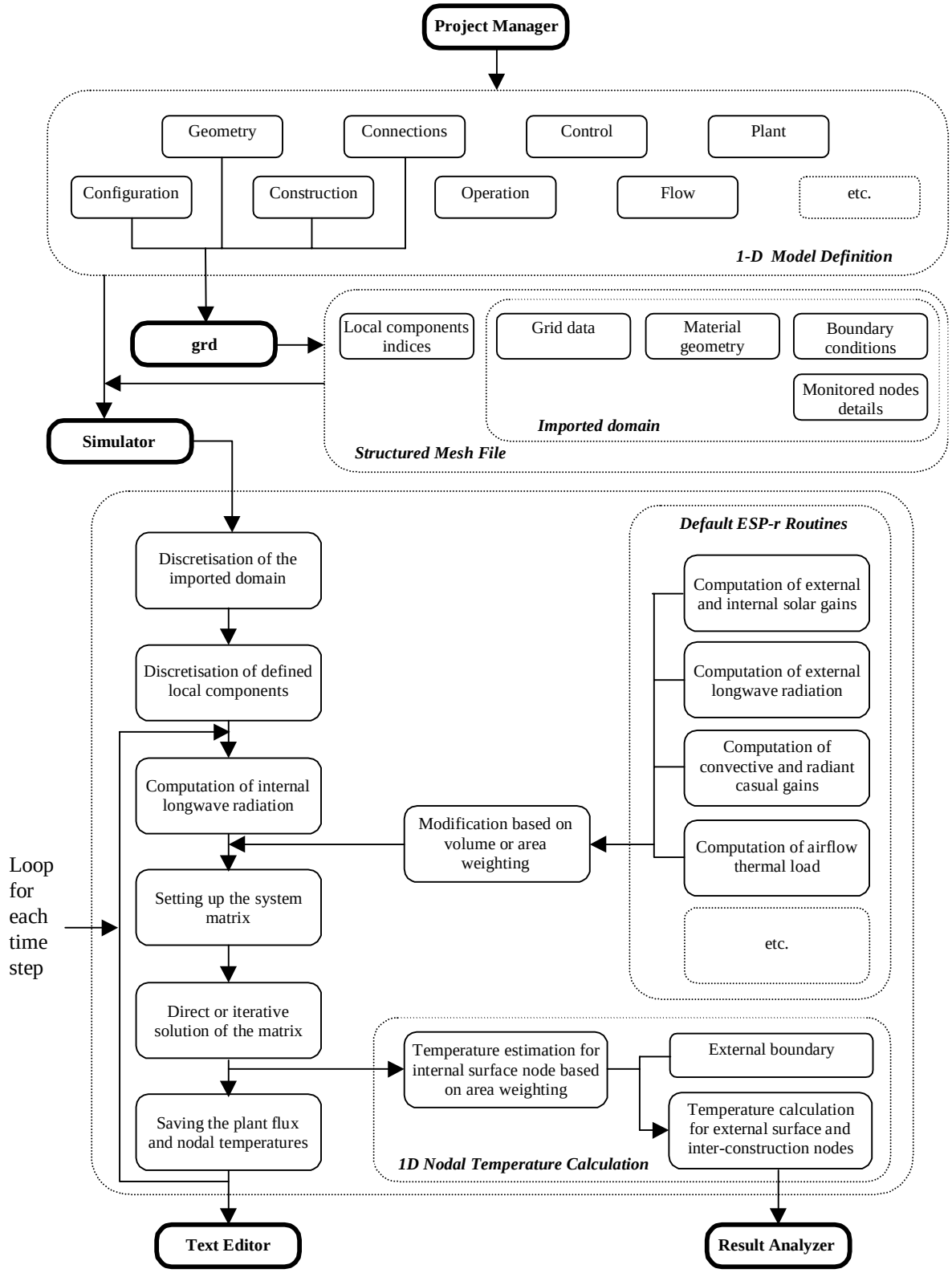

Figure 2. Schematic showing integration of the new module within the ESP-r simulation environment.

the internal surface nodes have one convection connection with the zone air node, and radiation connection with other internal surface nodes.

Furthermore, a climate data file defines the building external boundary variables.

With respect to the employed discretisation, a system matrix is created. In this matrix each node (i.e. 1D and 3D) is represented by one equation. These equations are then solved simultaneously with respect to the invoked control law. Two solution methods are available: direct and iterative. The iterative method is the default one, as it requires less storage space and it produces less round off errors. The adopted direct and iterative solution methods are Gauss's elimination method and the Gauss-Seidel method, respectively. The adopted Gauss-Seidel method incorporates linear under-relaxation factor.

For the defined local components, the default ESP-r space discretisation will be employed and their associated characteristic equations are created in the system matrix. The undefined local components will not be directly represented in the system matrix. They are replaced by the imported 3D domain. As in the 1D gridding, the internal surface nodes are connected with the space air node by convection, and connected with each other by radiation. For the internal radiation calculations, the 1D-view factors are employed after area weighting the 1D values and setting to zero the view factors between nodes within the same surface.

The fully implicit discretisation scheme is employed when the 3D modeling is invoked. This is because the fully implicit scheme is unconditionally stable, the coefficient generation process requires less CPU effort compared to other implicit schemes, and the amplification factor is always positive, hence prevents oscillation in the results, as shown in Figure 4.

Based on the results obtained from the 3D scheme, the default 1D temperatures are estimated either directly for the 1D constructions or by volume weighting for 3D constructions. This is because the 1D temperature distribution is required in the calculation of other thermal processes such as shortwave radiation, heat absorption by transparent materials, and convective heat transfer coefficient estimation.

At the result analyses level, the default options within the ESP-r environment, such as heat fluxes and temperature distribution can be used after 3D simulation. In addition, the new scheme allows monitoring the temperature profiles for several predefined nodes within the imported domain.

VALIDATION

In general, validation processes fall largely into three categories: analytical verification; inter-model comparison; and empirical validation. In analytic tests the predictions of programs are compared with exact analytical solutions. In empirical validation the results from thermal programs are compared with measurements made in buildings. In inter-model comparisons the predictions of a program are compared with those of other programs which, usually, are of similar sophistication.

The developed scheme was validated by inter-model and analytical verifications only, as no associated empirical validation data was available. In inter-model comparison, the results of the developed 3D module, which was integrated within the ESP-r, were compared against the ESP-r's default 1D analysis and VOLTRA[2] packages. First, the developed module was used to model transient 3D-heat flow through a building construction similar to the wall construction in Figure 3. The boundaries at the lateral directions were set to adiabatic. For the perpendicular direction, the internal ambient temperature was set to 24 °C, and the external boundary was defined by climate file of a typical meteorological year for Kuwait. Therefore, the defined problem was of 1D nature even though a 3D gridding was employed. The heat flow rate for the 3D problem were compared with that of an equivalent 1D model by ESP-r. The results matched up to two decimal digits.

For the other inter-model comparison, the developed module within the ESP-r was invoked to compare against VOLTRA modeling accuracy. The problem modeled by VOLTRA was transient heat conduction through the building corner shown in Figure 3. As shown in Figure 4 and Figure 5 the results agree with each other except for minor variations. The minor differences in the results were due to the difference in the discretisation schemes employed. While ESP-r is based on fully implicit scheme, VOLTRA incorporates Crank-Nicolson discretisation scheme. The oscillation in the VOLTRA results is due to the nature of stability error associated with the Crank-Nicolson discretisation scheme (Hensen and Nakhi 1994). For 10 minutes time step, the oscillations were significantly dampened and better agreement was obtained between the ESP-r and the VOLTRA. The

[2] VOLTRA is a tool developed by the Belgian company PHYSIBEL for 3D transient heat conduction modeling.

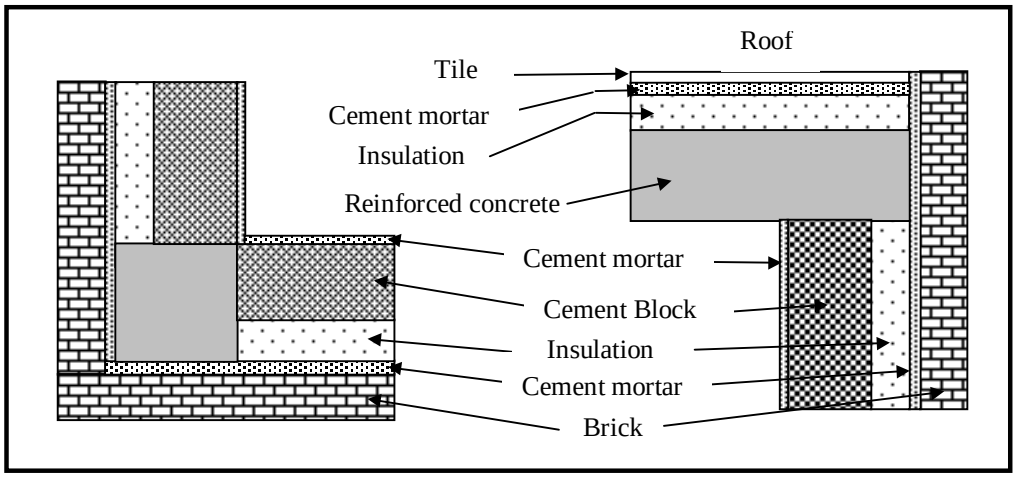

Figure 3: A schematic showing horizontal and vertical cross-sections of a corner

results were not shown since they almost overlap each other.

In the analytical verification, the results of ESP-r were compared with the exact solution of transient three-dimensional heat conduction through a homogeneous slab. For a rectangular parallelepiped domain ($0 \le x \le a$, $0 \le y \le b$, and $0 \le z \le c$) that is initially at 50 °C, and for times $t > 0$ the boundaries are defined by

$$-\lambda \frac{\partial T}{\partial x} + h_{out} T = 0 \qquad \text{at } x = 0 \qquad \textbf{(6a)}$$

$$\lambda \frac{\partial T}{\partial x} + h_{in} T = 0 \qquad \text{at } x = a \qquad \textbf{(6b)}$$

$$\frac{\partial T}{\partial y} = 0 \qquad \text{at } y = 0 \qquad \textbf{(6c)}$$

$$\lambda \frac{\partial T}{\partial y} + h_{y} T = 0 \qquad \text{at } y = b \qquad \textbf{(6d)}$$

$$\frac{\partial T}{\partial z} = 0 \qquad \text{at } x = 0 \qquad \textbf{(6e)}$$

$$\lambda \frac{\partial T}{\partial z} + h_{z} T = 0 \qquad \text{at } z = c \qquad \textbf{(6f)}$$

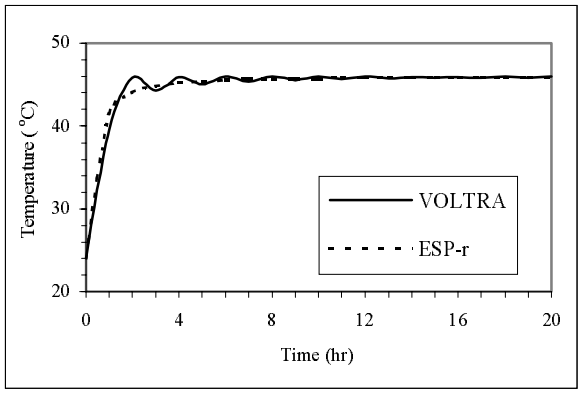

Figure 4: External corner temperature

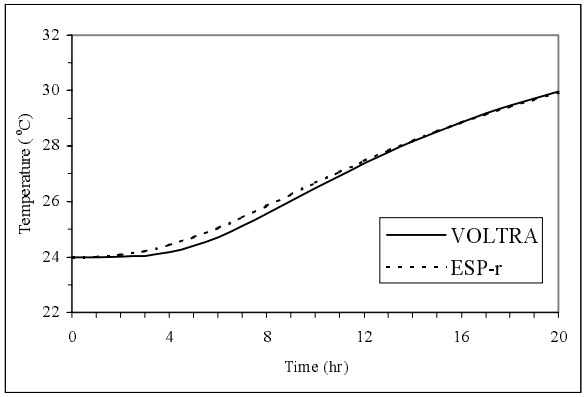

Figure 5: Internal corner temperature

Ozisik (1993) presented the general solution for multi-dimensional homogeneous heat conduction problems. For the current problem the solution can be written as

$$T(x,y,z,t) = 8T^* \sum\sum\sum e^{-\alpha\cdot\left(\beta_m^2+\gamma_n^2+\eta_p^2\right)t}$$

$$\times \frac{\left(\beta_m \cos(\beta_m x) + \frac{h_{out}}{\lambda}\sin(\beta_m x)\right)}{\left(\left(\beta_m^2 + \frac{h_{out}^2}{\lambda^2}\right)\cdot\left(a + \frac{h_{in}}{\lambda\cdot\left(\beta_m^2 + \frac{h_{in}^2}{\lambda^2}\right)}\right) + \frac{h_{out}}{\lambda}\right)}$$

$$\times \frac{\cos(\gamma_n y)\cdot\cos(\eta_p z)\cdot\left(\gamma_n^2 + \frac{h_y^2}{\lambda^2}\right)\cdot\left(\eta_p^2 + \frac{h_z^2}{\lambda^2}\right)}{\left(b\cdot\left(\gamma_n^2 + \frac{h_y^2}{\lambda^2}\right) + \frac{h_y}{\lambda}\right)\cdot\left(c\cdot\left(\eta_p^2 + \frac{h_z^2}{\lambda^2}\right) + \frac{h_z}{\lambda}\right)}$$

$$\times \frac{\left(\frac{h_{out}}{\lambda} + \beta_m\cdot\sin(\beta_m a) - \frac{h_{out}}{\lambda}\cos(\beta_m a)\right)}{\beta_m\cdot\gamma_n\cdot\eta_p}$$

$$\times \sin(\gamma_n b)\cdot\sin(\eta_p c) \qquad (7)$$

Where, the eigenvalues β_m, γ_n, and η_p are the positive roots of the following equations

$$\tan(\beta_m a) = \frac{\beta_m\left(h_{out}+h_{in}\right)}{\lambda\cdot\left(\beta_m^2 - \frac{h_{out}\cdot h_{in}}{\lambda^2}\right)} \qquad (8)$$

$$\gamma_n \tan(\gamma_n b) = \frac{h_y}{\lambda} \qquad (9)$$

$$\eta_p \tan(\eta_p c) = \frac{h_z}{\lambda} \qquad (10)$$

The results of the analytical validation based on 500 eigenvalues of each of β, γ, and η are shown in Figure 6. The temperature profiles shown are for the center node of the external surface. The reason for selecting the external surface is because of the expected highest truncation error due to the highest temperature gradient in the time direction. In addition, the stepwise excitation from 50 °C to 0 °C in the external ambient temperature was also intended to amplify the errors.

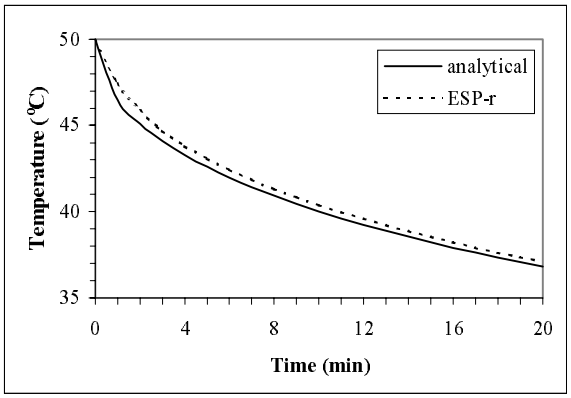

Figure 6: Comparison between analytical and ESP-r results

CONCLUSIONS

A new thermal bridging assessment module that was integrated within a state-of-the-art, whole building simulation environment was developed. The developed tool is distinguished by the flexibility in domain definition, and by the level of conflation with whole building simulation package, which facilitated more pragmatic boundary conditions for the domain under study.

In order to encourage the employment of the developed tool in practice, it was furnished with a user-friendly interface that is compatible with the whole building simulation package. In addition, both inter-model and analytical validations were performed to verify the adopted domain definition procedure. The tool was equipped with further user-friendly features such as the on-line help and exemplars.

REFERENCES

Clarke, J. A., 1985, *Energy Simulation in Building Design*, Adam Hilger Ltd., Bristol.

Clarke, J. A., 1994, Building Simulation: Realising the Potential, *Proceedings of the Building Environmental Performance*, U.K.

Hensen, J. L., and A. E. Nakhi, 1994, Fourier and Biot Numbers and the Accuracy of Conduction Modeling, *Proceedings of the Building Environmental Performance*, U.K.

Ozisik, M. N., 1993, *Heat Conduction*, John Wiley, USA.

Strachan, P. A., A. E., Nakhi, and C., Sanders, 1995, Thermal Bridging Assessments, *Proceedings of the Building Simulation `95*, U.S.A.

NOMENCLATURE

A	Area (m^2)
c_p	Specific heat (kJ/kg.K)
$\overline{g}$	Heat source term (W/m^3)
h_c	Convective heat transfer coefficient ($W/m^2.K$)
h_r	Radiative heat transfer coefficient ($W/m^2.K$)
N_b	Number of homogeneous boundary conditions.
N_m	Number of homogeneous materials in a control volume.
t	Time (s)
T	Temperature (°C).
T^*	Initial temperature (°C).
V	Volume (m^3)
x, y, z	Location in the x, y, and z directions (m)
ρ	Density (kg/m^3).
λ	Thermal conductivity (W/m.K).
β, γ, η	Eigenvalues.